



Explicit equations for the height and position of the first component shock for binary mixtures with competitive Langmuir isotherms under ideal conditions

Jani Siitonen, Tuomo Sainio*

Lappeenranta University of Technology, Skinnarilankatu 34, FIN-53850 Lappeenranta, Finland

ARTICLE INFO

Article history:

Received 14 April 2011

Received in revised form 24 June 2011

Accepted 1 July 2011

Available online 8 July 2011

Keywords:

Equilibrium theory

Ideal model

First component shock

Langmuir isotherm

ABSTRACT

Explicit equations for the height c_1^S and retention time $t_{R,1}$ of the pure first component shock in the case of a narrow rectangular injection pulse of a binary mixture with competitive Langmuir isotherms were derived within the frame of the equilibrium theory. The height of the first shock is obtained as an only positive root of a quartic equation. Hence, it was shown that, for binary Langmuir systems, the individual concentration profiles at the column outlet can be expressed entirely in closed-form. In addition, a novel, simple parametric representation that gives the trajectory of the first shock in the distance–time diagram as a function of c_1^S was derived. The practical relevance of the new equations was demonstrated by utilizing them for optimization of batch chromatography. It was shown that c_1^S increases and $t_{R,1}$ decreases with increasing duration of injection for given feed concentrations when the pure first component plateau is eroded during elution. The derivative of the cycle time with respect to the duration of injection is always more than unity. For this reason, the maximum productivity of more retained component is obtained when the duration of injection is selected so that the purity constraint can be fulfilled by having 100% yield. For the less retained component, an implicit expression for the maximum productivity was derived. When the injected loadings are constant, $t_{R,1}$ decreases with increasing feed concentrations while c_1^S and the cycle time are independent of them. In addition, the productivities of both components always increase with increasing feed concentrations.

© 2011 Elsevier B.V. All rights reserved.

1. Introduction

Preparative chromatography is a highly developed technique for many difficult separations in the pharmaceutical, fine chemical and food industries. Within these applications, chromatography is typically operated at overloaded conditions, for which nonlinear competitive adsorption behavior is characteristic. Under these conditions, the solute propagation in the column is essentially controlled by the thermodynamics of phase equilibria, while kinetic properties have a secondary, albeit not negligible, effect on the system dynamics [1].

For decades, different chromatographic systems have been described by using so called equilibrium theory of chromatography [1–9]. Within the frame of the theory, the propagation of the concentration states in the column are described by considering convection and phase equilibrium only, while mass transfer resistance and axial dispersion are neglected. The theory provides an understanding of the main features of the column dynamics, such as formation and propagation of concentration shocks, dispersive waves and their interactions for single, binary as well as multi-

component systems. It has been used widely for the analysis and design of both single-column [10–13] and multi-column chromatographic processes [14,15].

The equilibrium model consists of hyperbolic first-order partial differential equations. In the case of classical competitive Langmuir isotherms and piecewise constant boundary condition, the solution of the model equations can be given mostly in explicit form, also in the case of multi-component systems. First comprehensive analyses of the problem have been presented already in the 1940s by Devault [2] and by Glueckauf [3]. They both discussed the mathematical theory of the two-component problem and showed, for example, the existence of two discontinuities, one in front of each band. Later, Helfferich and Klein [1] and Rhee et al. [4] calculated the composition trajectories in the distance–time plane by exploiting two different approaches: so-called h -transform and the method of characteristics, respectively. Based on these approaches, Golshan-Shirazi and Guiochon [5,6] have presented an exact, analytical solution for almost the entire chromatographic cycle at column outlet in the case of a binary Langmuir system. However, in the case of small injection, they have been unable to derive a closed-form solution for the height of the pure first component shock c_1^S and for the retention time of the shock $t_{R,1}$. Recently, Rajendran and Mazzotti [9] have presented the trajectory of the first shock in the distance–time diagram in parametric form by using ω -transform,

* Corresponding author. Tel.: +358 5 62111; fax: +358 5 62199.

E-mail address: tuomo.sainio@lut.fi (T. Sainio).

but they have not discussed the solution at the column outlet. Closed-form equations for the height and position of the first shock have not been reported.

Lack of explicit equations for c_1^S and $t_{R,1}$ significantly complicates the analysis and design of chromatographic systems, especially the evaluation of the key performance parameters such as productivity and eluent consumption [10–13]. This is because the most useful definition of the cycle time allows “stacked injections” where the front of each injection profile touches (but does not overlap with) the tail of the preceding one. In absence of the complete closed-form solution of the chromatogram, the cycle time has even been defined excessively large in some optimization studies [10,11], which limits the practical relevance of the results. In addition, equations for the retention times of the shock fronts are needed to estimate adsorption isotherm parameters in a recently introduced experimental method [16].

The main objective of the present work is to derive a closed-form expression for the height and retention time of the pure first component shock in the case of a narrow rectangular injection pulse of a binary mixture with competitive Langmuir isotherm. The approach is based on the equilibrium theory of chromatography and it can be considered as a complement to the work of Golshan-Shirazi and Guiochon [5].

At the beginning of this contribution, the fundamentals of the equilibrium theory will be summarized. After that, analytic solutions for c_1^S and $t_{R,1}$ are derived. It will be shown that, for binary Langmuir systems, the individual concentration profiles at column outlet can be expressed entirely in closed-form. The obtained results are applied to derive a simple parametric representation for the trajectory of the first shock in the distance–time diagram. The location of the first shock in physical plane is given as a function of c_1^S . Finally, the practical relevance of the novel equations will be demonstrated by deriving differentials of c_1^S and $t_{R,1}$ with respect to typical operating parameters that can be varied in practical applications and by using them for optimization of batch chromatography.

2. Background

Within the frame of the equilibrium theory, the mass balance for an individual component i is written as

$$\frac{\partial}{\partial t}(c_i + Fq_i) + u \frac{\partial c_i}{\partial x} = 0 \quad (i = 1, 2) \quad (1)$$

where c_i and q_i are the mobile and the stationary phase concentrations of solute i , F is the phase ratio, t is time, x is the space coordinate, and u is the interstitial velocity. For binary systems that follow the competitive Langmuir adsorption isotherm model the equilibrium relationship is given by

$$q_i = \frac{q_{m,i} b_i c_i}{1 + b_1 c_1 + b_2 c_2} \quad (i = 1, 2) \quad (2)$$

where $q_{m,i}$ and b_i are the saturation capacity of the stationary phase and the Langmuir parameter of solute i , respectively. In the following discussion, it is assumed that component 1 is the less strongly adsorbed one. This means that $a_2 > a_1$, where $a_i = b_i q_{m,i}$ is the Henry constant of component i .

Eqs. (1) and (2) form a coupled system of two first-order partial differential equations. The system can be solved by the method of characteristics when Riemann boundary conditions are used. Typically, the task is to describe the solute propagation in the column when a rectangular pulse of binary mixture with known duration, Δt_{inj} , is first injected to an initially clean column and then eluted. In this case, the initial and boundary conditions of Eq. (1) are

$$c_i(x, t = 0) = 0 \quad \text{for } 0 \leq x \leq L \quad (3)$$

$$c_i(x = 0, t) = c_i^F \quad \text{for } 0 \leq t \leq \Delta t_{inj} \quad (4)$$

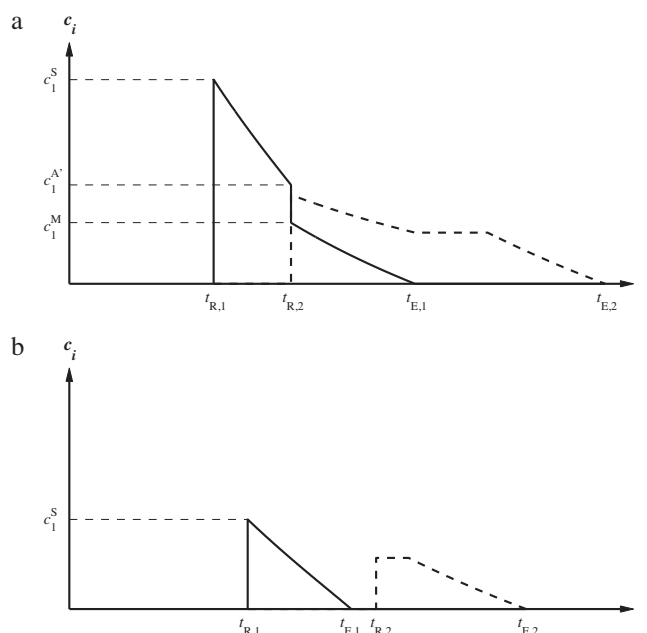


Fig. 1. Individual elution profiles of a rectangular injection pulse at the column outlet. (a) Incomplete separation. Conditions: $c_1^F = c_2^F = 10$ g/L; $q_{m,1} = q_{m,2} = 100$ g/L; $b_1 = 0.02$ L/g; $b_2 = 0.025$ L/g; $F = 1/3$; $V_{inj} = 0.1$ bed volumes. (b) Complete separation. Same conditions as for (a) except $V_{inj} = 0.03$ bed volumes.

$$c_i(x = 0, t) = 0 \quad \text{for } t > \Delta t_{inj} \quad (5)$$

where L is the column length and c_i^F is the concentration of component i in feed.

If the injection is wide enough, the pure component 1 plateau in the front of the elution profile is not eroded during elution, and the individual concentration profiles at the column outlet can be expressed entirely in closed form [5]. However, for sufficiently small injections, the plateau erodes completely, and the height of the front shock decreases while it propagates through the column. For such a case, no closed-form expression has been presented for the height or retention time of the first pure component shock. The distance from the column inlet, where the pure first component plateau is eroded completely, is given by

$$x_E = \frac{u(1 + b_1 c_1^A)^2 \Delta t_{inj}}{F a_1 b_1 c_1^A} \left[1 - \frac{\beta b_2 c_2^F}{\alpha(\beta + b_1 c_1^A)^2} \right] \quad (6)$$

where $\alpha = a_2/a_1$ is the separation factor, $\beta = 1 - 1/\alpha$ is an auxiliary parameter, $c_1^A = c_1^F [1 + b_2/(\alpha b_1 \xi_+)]$ is the height of the first shock before erosion, and ξ_+ is the slope of Γ_+ characteristic corresponding the feed composition whose value can be calculated explicitly from adsorption isotherm parameters [8].

Typical elution profiles in the case of a narrow injection pulse are illustrated in Fig. 1. Depending on the resolution between the bands there are two possibilities. Fig. 1a represents the case where the components are not separated completely. The concentration profiles at column outlet consist of three zones. A zone of pure first component elutes between times $t_{R,1}$ and $t_{R,2}$, a mixed zone between $t_{R,2}$ and $t_{E,1}$, and a zone of pure second component between $t_{E,1}$ and $t_{E,2}$. In the case of complete separation, illustrated in Fig. 1b, there is no mixed zone left. The main features of the solution are a concentration shock in the front of both bands, a pure diffuse boundary for both components and a possible second component concentration plateau.

If the components are not separated completely (Fig. 1a), the retention time of the second shock $t_{R,2}$ and the end of elution profile

of the first component $t_{E,1}$ are given by [5]

$$t_{R,2} = \Delta t_{inj} + t_0 \left[1 + Fa_2 \gamma \left(1 - \sqrt{L'_f} \right)^2 \right] \quad (7)$$

$$t_{E,1} = \Delta t_{inj} + t_0 \left(1 + \frac{\gamma Fa_1}{\alpha} \right) \quad (8)$$

In the above equations, t_0 is the elution time of a non-retained component, $L_{f,2} = (b_2 c_2^F \Delta t_{inj}) / (Fa_2 t_0)$ is the loading factor of the second component, and $L'_f = (1 + \xi_+ b_1 / b_2) L_{f,2}$ and $\gamma = (\alpha b_1 \xi_+ + b_2) / (b_1 \xi_+ + b_2)$ are auxiliary parameters.

The concentration profile of the first component in mixed zone (between $t_{R,2}$ and $t_{E,1}$) is given by

$$c_1 = \frac{1}{b_1 + b_2 / (\alpha \xi_+)} \left[\sqrt{\frac{\gamma}{\alpha} \frac{t_0 Fa_1}{t - \Delta t_{inj} - t_0}} - 1 \right] \quad (9)$$

and in the pure first component zone (between $t_{R,1}$ and $t_{R,2}$) by

$$t = \Delta t_{inj} + t_0 + t_0 Fa_1 \left[\frac{1}{(1 + b_1 c_1)^2} - L_{f,2} \frac{\beta}{(\beta + b_1 c_1)^2} \right] \quad (10)$$

It should be noted that the latter equation gives elution time as a function of c_1 , while there is no closed-form solution giving the relationship the other way around. This is the very reason that has complicated the derivation of a complete analytic solution for the ideal model of chromatography. The first component concentration at the rear of the second shock c_1^M (see Fig. 1a) is obtained from Eq. (9) by setting $t = t_{R,2}$

$$c_1^M = \frac{\alpha \xi_+}{b_2 + \alpha b_1 \xi_+} \frac{\sqrt{L'_f} - \beta}{1 - \sqrt{L'_f}} \quad (11)$$

and at the front of the second shock $c_1^{A'}$ from Eq. (10)

$$c_1^{A'} = \frac{\sqrt{L'_f} - \beta}{b_1 (1 - \sqrt{L'_f})} \quad (12)$$

For the retention time of the first shock $t_{R,1}$, there has not been a closed-form solution so far. For solving this problem Golshan-Shirazi and Guiochon [5] have provided a numerical approach. Alternatively, $t_{R,1}$ can be solved from the parametric representation given by Rajendran and Mazzotti [9].

In the case of complete separation (Fig. 1b), the mixed zone has disappeared and the rear diffuse profile of the first component can be calculated entirely by Eq. (10). The end time of the profile is given by

$$t_{E,1} = \Delta t_{inj} + t_0 + t_0 Fa_1 \left(1 - \frac{L_{f,2}}{\beta} \right) \quad (13)$$

As in the case of incomplete separation, there has been no method for solving the height or the retention time of the front shock in closed-form, but the above mentioned numerical approaches can be applied.

3. Closed-form equations for the height and retention time of the first shock

A closed-form solution for the height and retention time of the first component shock is derived as follows. As in the numerical method by Golshan-Shirazi and Guiochon [5], the idea is to utilize mass balance of the first component to calculate first c_1^S and then $t_{R,1}$.

Although the elution profile of the pure first component (Eq. (10)) cannot be presented in closed-form such that it gives c_1 as a function of time, the mass of the first component eluted from the

column can be calculated as a function of c_1^S . This is obtained by integrating the elution profile piecewise with respect to c_1 from 0 to c_1^S and by subtracting $c_1^S t_{R,1}$ from the value of the integral. The calculation principle is presented in Fig. 2. The areas of hatched regions A_3 – A_5 correspond to the values of the integral terms, the area of dark grey region A_1 to the amount of component 1, and the area of light grey region A_2 to the difference between these values.

In the case of incomplete separation (Fig. 2a), the mass balance can be written as

$$c_1^F \Delta t_{inj} = A_1 = A_5 + A_4 + A_3 - A_2 = \int_0^{c_1^M} t \, dc_1 + \int_{c_1^M}^{c_1^{A'}} t \, dc_1 + \int_{c_1^S}^{c_1^M} t \, dc_1 - c_1^S t_{R,1} = \frac{t_0 Fa_1}{b_1} \left(\frac{b_1 c_1^S}{1 + b_1 c_1^S} \right)^2 - \left\{ \frac{\alpha b_2 c_2^F}{b_1} \left[\frac{b_1 c_1^S}{\alpha(1 + b_1 c_1^S) - 1} \right]^2 \right\} \Delta t_{inj} \quad (14)$$

and in the case of complete separation (Fig. 2b) as

$$c_1^F \Delta t_{inj} = A_1 = A_3 - A_2 = \int_0^{c_1^S} t \, dc_1 - c_1^S t_{R,1} = \frac{t_0 Fa_1}{b_1} \left(\frac{b_1 c_1^S}{1 + b_1 c_1^S} \right)^2 - \left\{ \frac{\alpha b_2 c_2^F}{b_1} \left[\frac{b_1 c_1^S}{\alpha(1 + b_1 c_1^S) - 1} \right]^2 \right\} \Delta t_{inj} \quad (15)$$

It is interesting to note that both cases lead to exactly the same result. By dividing the both sides of Eq. (14) or Eq. (15) by $c_1^F \Delta t_{inj}$ and by simplifying the resulting equation, the following implicit expression for c_1^S is obtained:

$$L_{f,1} \left(1 + \frac{1}{b_1 c_1^S} \right)^2 + L_{f,2} \left(1 + \frac{1}{\alpha(1 + b_1 c_1^S) - 1} \right)^2 = 1 \quad (16)$$

As seen in Eq. (16), the height of first component shock depends only on the loading factors, the separation factor and the Langmuir parameter of the first component. The concentration c_1^S can be solved by re-arranging the above equation to give

$$A(b_1 c_1^S)^4 + B(b_1 c_1^S)^3 + C(b_1 c_1^S)^2 + Db_1 c_1^S + E = 0 \quad (17)$$

where

$$A = L_{f,1} + L_{f,2} - 1 \quad (18)$$

$$B = 2[L_{f,1} + L_{f,2} + \beta(L_{f,1} - 1)] \quad (19)$$

$$C = L_{f,1} + L_{f,2} + \beta[4L_{f,1} + \beta(L_{f,1} - 1)] \quad (20)$$

$$D = 2L_{f,1} \beta(\beta + 1) \quad (21)$$

$$E = L_{f,1} \beta^2 \quad (22)$$

Eq. (17) is a quartic equation with respect to $b_1 c_1^S$. It can be solved analytically, for example by using Ferrari's method [17], Descartes–Euler method [18] or Neumark's method [19]. In Appendix A, it is shown that, when $\alpha > 1$, $L_{f,1} > 0$, and $L_{f,2} > 0$, Eq. (17) has only one positive real root. This root must give the height of the first shock. Applicability of different algorithms for solving Eq. (17) is discussed in the next section.

Once c_1^S is obtained, the retention time of the first shock can be calculated from Eq. (10) by setting $c_1 = c_1^S$. An alternative form,

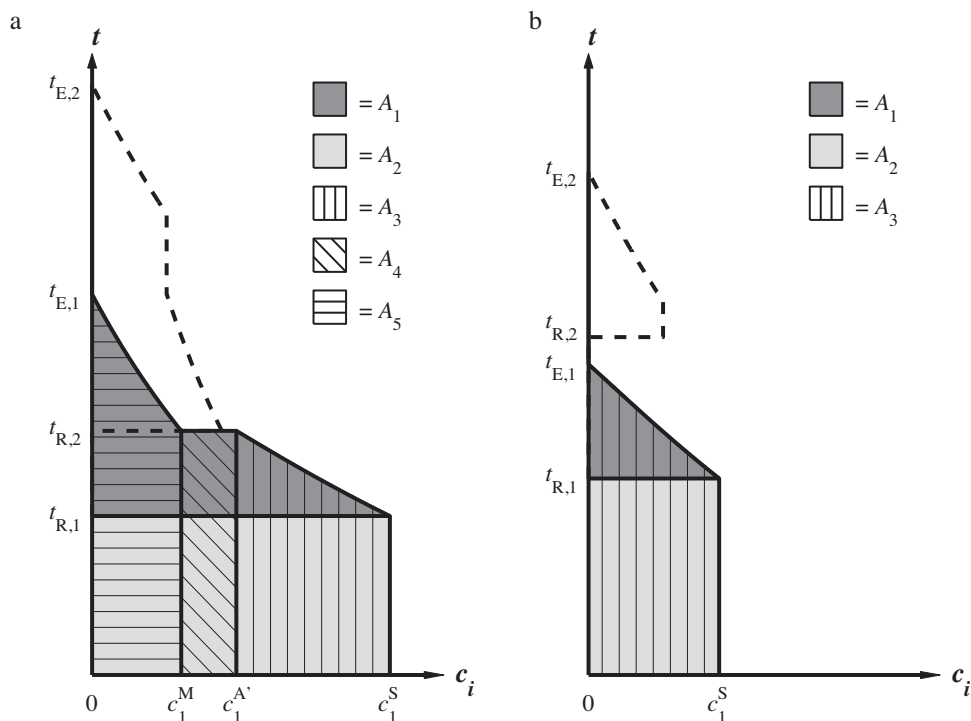


Fig. 2. Individual elution profiles of a rectangular injection pulse presented in the concentration–time coordinate system. A_1 , the total amount of component 1. A_2 , the difference between the sum of integral terms A_3 – A_5 and the total amount of component 1. A_3 – A_5 , integral terms in Eqs. (14) and (15). Same conditions as in Fig. 1.

where $t_{R,1}$ is expressed as a function of $L_{f,1}$, is obtained by combining Eqs. (10) and (16)

$$t_{R,1} = \Delta t_{inj} + t_0 + t_0 Fa_1 \left[\frac{1}{\alpha(1 + b_1 c_1^S)^2} + L_{f,1} \frac{\beta}{(b_1 c_1^S)^2} \right] \quad (23)$$

Finally, it should be noted that closed-form equations for the height and retention time of the first shock can be obtained also by using another approach. Rajendran and Mazzotti [9] have recently derived a parametric representation of the trajectory of the first shock by using the ω -transform. Although not pursued by Rajendran and Mazzotti, it is straightforward to show that their equations also lead to a quartic when solved for characteristic parameter ω_1^S which corresponds to the shock height. Unfortunately, the solution is more complex than the one presented here. A somewhat simpler form is obtained by substituting loading factors into the parametric representation of Rajendran and Mazzotti, but this will not be discussed here.

4. Solution of the quartic equation

Several analytic algorithms have been published to solve quartic equations [17–19]. However, as to the computational implementation, none of them is unconditionally stable with arbitrary parameters. The methods have different properties with regard to overflow and round-off errors. Physical constraints pose the following limits for the coefficients of Eq. (17): $-1 < A < 0$, $-2 < B < 2$, $-1 < C < 5$, $0 < D < 4$, $0 < E < 1$. The question arises, which algorithm is best suited for solving this quartic equation?

A Matlab code was developed to compare the following four algorithms: (1) Ferrari's solution [17], (2) Descartes–Euler solution [18], (3) Neumark's solution [19], and (4) the solution given by Matlab's Symbolic Math Toolbox. Ten million random combinations of parameters $L_{f,1}$, $L_{f,2}$, and α , were examined with all algorithms. The accuracy of each solution was checked by substituting the obtained positive root c_1^{S*} back into the left hand side of Eq. (16) and by

calculating the relative residual defined as

$$res = \left| \frac{1 - f(c_1^{S*})}{1} \right| \quad (24)$$

According to the simulations, the most applicable option for solving Eq. (17) is the Ferrari's solution. With this algorithm, the relative residual was always less than 32×10^{-12} . However, also the Descartes–Euler solution and the Neumark's solution were observed to be relatively stable. The maximum relative residual with the Descartes–Euler solution was 0.45×10^{-6} and with the Neumark's solution 0.24×10^{-3} .

In contrast to the other methods, the Matlab's symbolic solution was not completely stable. The maximum residual was 0.80, and in 1413 cases out of ten million the relative residual was more than 1%. In addition, in 616 cases a root was not obtained at all, because the round-off errors led to an indeterminate form 0/0. For example, with parameters $L_{f,1} = 0.028$, $L_{f,2} = 0.067$ and $\alpha = 1.4$ the relative residual was 4.3% and with parameters $L_{f,1} = 0.031$, $L_{f,2} = 0.243$ and $\alpha = 2.0$ no root was obtained. In the former case, the retention time of the first shock calculated by Eq. (10) was 0.85% too large, when $\Delta t_{inj}/t_0 = 0.1$ and $Fa_1 = 4.5$. In addition, the Matlab solution was about one hundred times slower than the other ones. This is not a major factor, however, since the calculation time of one root was always less than 5 ms on a standard desktop computer.

The recommended Ferrari's algorithm is given in Table 1. The idea is to first solve one root of a particular cubic equation (I.1), the coefficients of which are obtained from those of the original quartic equation. This root is then used to factorize the quartic into two quadratics that can be solved.

In Eqs. (I.4) and (I.5) $\sqrt{\quad}$ and $\sqrt[3]{\quad}$ stand for any determination of the square or cubic root. However, it was observed that the algorithm is most stable when the principal cubic root is used. In addition, it is recommended to select the sign of Q opposite to the sign of m .

As mentioned in Section 3, Eq. (17) has only one positive real root. In addition, it is shown in Appendix A that Eq. (17) does not

Table 1
Ferrari's algorithm for solving a quartic equation [17].

The subsidiary cubic equation	
$y^3 + ky + m = 0$	(1.1)
$k = \frac{BD}{A^2} - \frac{C^2}{3A^2} - \frac{4E}{A}$	(1.2)
$m = \frac{BCD}{3A^3} - \frac{2C^2}{27A^3} - \frac{D^2}{A^2} - \frac{B^2E}{A^3} + \frac{8CE}{3A^2}$	(1.3)
A root of the cubic equation	
$y = \frac{\sqrt[3]{Q - 108m}}{6} - \frac{2k}{\sqrt[3]{Q - 108m}}$	(1.4)
$Q = 12\sqrt{12k^3 + 81m^2}$	(1.5)
The four roots of the original quartic equation (17)	
$(b_1c_1^S)_1 = -\frac{B}{4A} + \frac{R}{2} + \frac{\sqrt{S+T/R}}{2}$	(1.6)
$(b_1c_1^S)_2 = -\frac{B}{4A} + \frac{R}{2} - \frac{\sqrt{S+T/R}}{2}$	(1.7)
$(b_1c_1^S)_3 = -\frac{B}{4A} - \frac{R}{2} + \frac{\sqrt{S-T/R}}{2}$	(1.8)
$(b_1c_1^S)_4 = -\frac{B}{4A} - \frac{R}{2} - \frac{\sqrt{S-T/R}}{2}$	(1.9)
$R = \sqrt{\frac{B^2}{4A^2} - \frac{2C}{3A} + y}$	(1.10)
$S = \frac{B^2}{2A^2} - \frac{4C}{3A} - y$	(1.11)
$T = \frac{BC}{A^2} - \frac{B^3}{4A^3} - \frac{2D}{A}$	(1.12)

have any complex root with positive real part. For these reasons, the right root is always the one having the largest real part. The right solution is given by Eq. (1.6), if

$$\text{Re}(2R) > \text{Re} \left(\sqrt{S - \frac{T}{R}} - \sqrt{S + \frac{T}{R}} \right) \quad (25)$$

and otherwise by Eq. (1.8). It was observed in the numerical tests performed that the above inequality held true for every set of parameters when the principal cubic root was used in Eq. (1.4), and the correct root was always obtained from Eq. (1.6).

5. Construction of the distance–time diagram

The solute movement in a chromatography column is conveniently presented in a distance–time diagram. In such a diagram, composition variables are shown as contour lines in a two-dimensional coordinate system with distance from the column inlet x as one coordinate and time t as the other. An example of the distance–time diagram is shown in Fig. 3.

The moment, when the pure first component plateau is eroded completely, is indicated in Fig. 3 by point E. Beyond this point, the height of first shock decreases and the velocity of the shock decelerates. Graphically this means that the trajectory of the first shock S_1 is no longer a straight line but is curved upwards.

It is obvious that, since the retention time of the first shock at column outlet can be expressed explicitly as described in Section 3, also the location of the first component shock in the distance–time diagram can be obtained in closed form. This is observed by considering that the column length can be varied and the corresponding time calculated by Eq. (10). However, because the analytic solution for $t_{R,1}$ is relatively complicated, a more convenient method to create the trajectory of the first shock on the distance–time diagram in parametric form as a function of c_1^S was derived. The method is a simpler alternative to the methods by Rhee et al. [8] and by Rajendran and Mazzotti [9].

At the point E, the height of first component shock has not yet decreased, and c_1^S is given by $c_1^S = c_1^A$. As the distance and time increase, c_1^S decreases and approaches zero when x and t approach

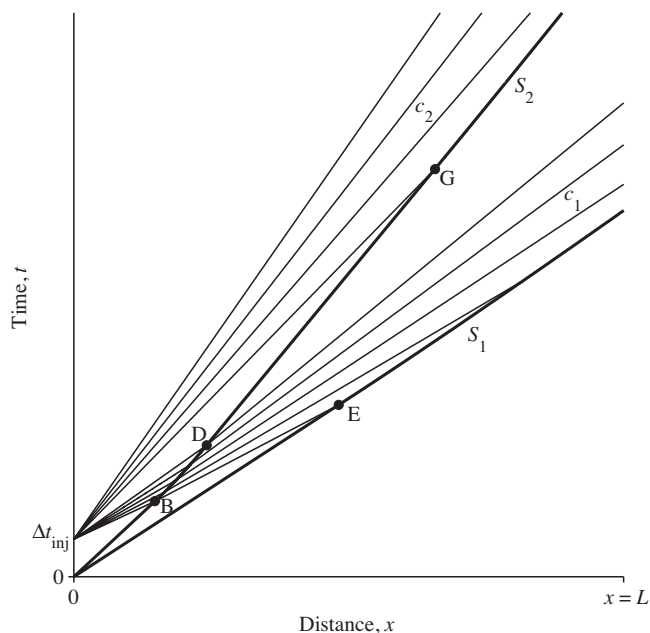


Fig. 3. Propagation of concentration states in the distance–time diagram for an arbitrary system. B, feed plateau is eroded; D, components are separated completely; E, pure first component plateau is eroded; G, pure second component plateau is eroded; S_1 , first shock; S_2 , second shock.

infinity. The distance x , where a given c_1^S is found in the column, can be calculated by using the global mass balance of the first component

$$\frac{x}{L} = L_{f,1} \left(1 + \frac{1}{b_1c_1^S} \right)^2 + L_{f,2} \left(1 + \frac{1}{\alpha(1 + b_1c_1^S) - 1} \right)^2 \quad (26)$$

It should be noted that Eq. (26) is equal to Eq. (16) at the column outlet where $x=L$.

The corresponding time $t_{R,1}$ can be solved by applying Eq. (10):

$$t_{R,1} = \left\{ 1 - \frac{(\alpha - 1)b_2c_2^F}{[\alpha(1 + b_1c_1^S) - 1]^2} \right\} \Delta t_{inj} + \frac{x}{L} \left[1 + \frac{Fa_1}{(1 + b_1c_1^S)^2} \right] t_0 \quad (27)$$

Eq. (27) gives time $t_{R,1}$ as a function of c_1^S and x . The latter parameter can be eliminated by substituting Eq. (26) to Eq. (27) which yields

$$t_{R,1} = \left\{ 1 + \frac{b_1c_1^F}{(b_1c_1^S)^2} \left[1 + \frac{(1 + b_1c_1^S)^2}{Fa_1} \right] + \frac{b_2c_2^F}{[\alpha(1 + b_1c_1^S) - 1]^2} \left[1 + \frac{\alpha^2(1 + b_1c_1^S)^2}{Fa_2} \right] \right\} \Delta t_{inj} \quad (28)$$

Hence, the trajectory of the first shock S_1 can be constructed by giving c_1^S values from c_1^A to 0 and calculating the corresponding x and t from Eqs. (26) and (28).

6. Demonstration of the practical relevance of the novel equations

The novel analytic equations, derived in Section 3, can be used to calculate differentials of c_1^S and $t_{R,1}$ with respect to typical operating parameters that can be varied in practical applications. Next, such derivatives will be derived and utilized in optimization of batch chromatography in two different cases. First, the effect of the duration of injection on c_1^S , $t_{R,1}$, and the main process performance parameters is investigated when the feed concentrations c_1^F and c_2^F

are constant. Secondly, the total feed concentration will be varied while keeping the injected loadings $L_{f,1}$ and $L_{f,2}$ constant. The purpose is to demonstrate that the novel analytic equations have also practical relevance. It should be noted that the following discussion is limited to the case where the shock is eroded during elution, *i.e.* narrow injections, because the height of the shock, and hence its propagation velocity, is constant for sufficiently large injections.

6.1. Purification strategy

In this work, it is assumed that one or other of the components of a binary mixture is purified to a given purity constraint. The first component is the target constituent in the product fraction A, and the second component in the product fraction B. The purities of the product fractions are given by

$$p^A = \frac{m_1^A}{m_1^A + m_2^A} = \frac{\int_{t_{R,1}}^{t_{cut}} c_1 dt}{\int_{t_{R,1}}^{t_{cut}} (c_1 + c_2) dt} \quad (29)$$

$$p^B = \frac{m_2^B}{m_1^B + m_2^B} = \frac{\int_{t_{cut}}^{t_{E,2}} c_2 dt}{\int_{t_{cut}}^{t_{E,2}} (c_1 + c_2) dt} \quad (30)$$

where t_{cut} is the cut time at which the collection of the first fraction ends and the collection of second fraction begins.

The most common performance parameters of chromatographic processes are productivity PR , specific eluent consumption EC , and recovery yield Y . The focus of this work is on the productivity and the specific eluent consumption. This is because the complete analytic solution of the elution profiles allows using more a realistic definition of the cycle time than in previous studies. However, also the yield is discussed briefly, because it has an influence on the total separation costs. The performance parameters are here defined for component 1 (and analogously for component 2) as follows:

$$Y_1 = \frac{m_1^A}{m_1^F} = \frac{\int_{t_{R,1}}^{t_{cut}} c_1 dt}{m_1^F} \quad (31)$$

$$PR_1 = \frac{m_1^A}{\Delta t_{cycle}} \quad (32)$$

$$EC_1 = \frac{V_{eluent}}{m_1^A} = \frac{(\Delta t_{cycle} - \Delta t_{inj})\dot{V}}{m_1^A} \quad (33)$$

where Δt_{cycle} is the cycle time and V_{eluent} is the amount of eluent used in a chromatographic cycle.

The cycle time is here defined by assuming that no gap exists between consecutive chromatographic cycles. This means that the first component of the $(n+1)$ th injection begins to elute just after the second component of the n th injection has left the column:

$$\Delta t_{cycle} = t_{E,2} - t_{R,1} \quad (34)$$

The definition is different from the one used in many earlier optimization studies, where the effect of $t_{R,1}$ on the cycle time has not been taken account. For example, Golshan-Shirazi and Guiochon [10,11] have calculated the cycle time as the corrected analytical retention time of the second component $\Delta t_{cycle} = t_{E,2}^0 - t_0$, where $t_{E,2}^0$ is the retention time of the second component at infinite dilution. In practice, the definition used in this work is more relevant, because it gives the minimum cycle time required for consecutive, isocratic injections. As will be shown shortly, the definition of the cycle time affects significantly the optimization results.

6.2. Effect of the duration of injection on c_1^S , $t_{R,1}$ and Δt_{cycle}

One of the most typical practical problems with regard to batch chromatography is to find the duration of injection that leads to

optimal process performance, *i.e.* to minimum separation costs. Next, the effect of Δt_{inj} on c_1^S , $t_{R,1}$, Δt_{cycle} , and the process performance will be analyzed in the case of constant feed concentrations.

The derivative of c_1^S is obtained by differentiating Eq. (16) implicitly with respect to Δt_{inj}

$$\left. \frac{\partial c_1^S}{\partial \Delta t_{inj}} \right|_{c_1^F, c_2^F} = \left\{ 2b_1(1 + b_1 c_1^S) \left[\frac{L_{f,1}}{(b_1 c_1^S)^3} + \frac{L_{f,2}}{\alpha(\beta + b_1 c_1^S)^3} \right] \Delta t_{inj} \right\}^{-1} > 0 \quad (35)$$

As seen in the above equation, the height of the first shock at column outlet always increases with increasing Δt_{inj} . This is reasonable, because the larger the injection is, the later the first shock begins to erode as seen in Eq. (6). In addition, when Δt_{inj} increases, the height of the first shock must increase at every point of the column beyond the beginning of the shock erosion x_E (see Fig. 3). This is because Eq. (35) is valid for every column length $L > x_E$.

The corresponding derivative of the retention time $t_{R,1}$ is obtained by differentiating Eq. (10) with respect to Δt_{inj} , setting $c_1 = c_1^S$, and by substituting Eq. (35) to the resulting equation

$$\left. \frac{\partial t_{R,1}}{\partial \Delta t_{inj}} \right|_{c_1^F, c_2^F} = 1 - \frac{t_0 F a_1}{\Delta t_{inj}} \left\{ \frac{(1/(1 + b_1 c_1^S)^3) - (\beta L_{f,2}/(\beta + b_1 c_1^S)^3)}{[(L_{f,1}/(b_1 c_1^S)^3) + (L_{f,2}/\alpha(\beta + b_1 c_1^S)^3)] (1 + b_1 c_1^S)} + \frac{\beta L_{f,2}}{(\beta + b_1 c_1^S)^2} \right\} \quad (36)$$

On the basis of the right hand side of Eq. (36), it is not possible to say anything about the sign of the above derivative. However, the sign can be deduced by examining the shock height. As mentioned earlier, the shock height is independent of the duration of injection before the beginning of the shock erosion, x_E , and is the higher the larger the injection is beyond x_E . In addition, it is well known that the shock propagates the faster the higher it is. For these reasons, the first shock must reach the column outlet the earlier the larger the injection is, and the above derivative must therefore always be negative.

The derivative of the cycle time is obtained by differentiating Eq. (34). It is well known that the derivative of $t_{E,2}$ with respect to Δt_{inj} is always unity [12]. For this reason, the derivative of the cycle time must always be greater than unity

$$\left. \frac{\partial t_{cycle}}{\partial \Delta t_{inj}} \right|_{c_1^F, c_2^F} = 1 - \frac{\partial t_{R,1}}{\partial \Delta t_{inj}} > 1 \quad (37)$$

6.3. Effect of the duration of injection on the process performance

The optimum values of the operating parameters depend much on whether one is interested in purifying the first or the second eluted component [10]. When the second component is the target, the mass of the product fraction m_2^B is independent of Δt_{inj} , provided that the injection is large enough for matching the purity requirement without collecting the pure first component to the product fraction B [10]. This means that the productivity always decreases when the duration of injection increases due to increasing cycle time:

$$\frac{\partial PR_2}{\partial \Delta t_{inj}} = - \frac{m_2^B}{(\Delta t_{cycle})^2} \frac{\partial \Delta t_{cycle}}{\partial \Delta t_{inj}} < 0 \quad (38)$$

The specific eluent consumption increases, when Δt_{inj} increases. This is observed by differentiating Eq. (33), where the subscripts have been changed for component 2, which yields

$$\frac{\partial EC_2}{\partial \Delta t_{inj}} = \frac{\dot{V}}{m_2^B} \left(\frac{\partial \Delta t_{cycle}}{\partial \Delta t_{inj}} - 1 \right) > 0 \quad (39)$$

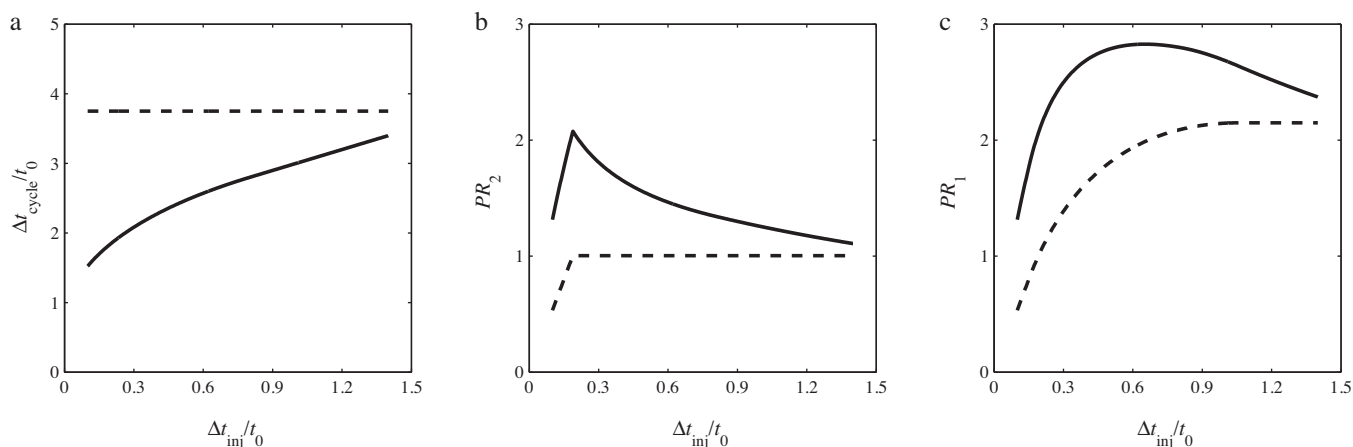


Fig. 4. Effect of the definition of the cycle time on the productivity. Solid lines: the cycle time is defined as $\Delta t_{\text{cycle}} = t_{E,2} - t_{R,1}$. Dotted lines: the cycle time is defined as $\Delta t_{\text{cycle}} = t_{E,2}^0 - t_0$. Conditions: $c_1^F = c_2^F = 20 \text{ g/L}$; $q_{m,1} = q_{m,2} = 100 \text{ g/L}$; $b_1 = 0.02 \text{ L/g}$; $b_2 = 0.025 \text{ L/g}$; $F = 1/3$; $p^A = p^B = 0.98$.

In addition, it has been shown that the yield of the component 2 decreases when Δt_{inj} increases [10]. This means that the optimum duration of injection is always such that the yield of the second component is 100% and the cut time is equal to the retention time of the second shock.

For the first component, the amount of the product m_1^A increases when Δt_{inj} increases [10]. This means that both the numerator and the denominator of Eq. (32) increase simultaneously. Hence, the analysis of the productivity of the first component is not as straightforward as for the second component. However, it can be shown that the productivity of the first component always goes through a maximum when Δt_{inj} increases. The maximum is achieved when the derivative of the productivity with respect to the Δt_{inj} is zero. An implicit expression for the zero point of the derivative is presented in Appendix B.

Because the derivative of the cycle time is greater than unity (see Eq. (37)), V_{eluent} increases with increasing Δt_{inj} . The minimum specific eluent consumption of the first component can be calculated by using a similar approach than for the maximum productivity. In addition, the yield decreases rapidly with Δt_{inj} [10]. For these reasons, the economic optimum might not be where the productivity is highest. Such calculations are beyond the scope of this work, however.

The influence of the definition of the cycle time on the productivity is illustrated in Fig. 4. The solid lines represent the definition used in this work, Eq. (34). The dashed lines are calculated by defining the cycle time as the corrected analytical retention time of the second component, as suggested by Golshan-Shirazi and Guiochon [10,11]. As seen in Fig. 4a, the definition used in this work gives significantly shorter cycle times than the other alternative and therefore higher productivities (Figs. 4b and c).

It is observed in Fig. 4b that the productivity of the second component first increases with increasing Δt_{inj} regardless the definition of the cycle time. In this region, the resolution between bands is so high that a portion of the pure first component fraction has to be collected in the product fraction B to fulfill the purity constraint. After the yield begins to fall below 100%, PR_2 levels off, if the cycle time is defined as the corrected analytical retention time of the second component. In contrast, with the definition of the cycle time used in this work, the larger the injection, the longer the cycle time is. The productivity of the second component thus decreases for large injections.

For the first component, both the maximum productivity and Δt_{inj} with which it is obtained differ significantly (Fig. 4c). In fact, when the cycle time is defined as the corrected analytical retention time of the second component, the productivity always increases

with Δt_{inj} until it levels off as the injection becomes so large that t_{cut} is located on the feed plateau. This gives a misleading impression that excessively large injections should be preferred.

6.4. Effect of the total feed concentration on c_1^S , $t_{R,1}$ and Δt_{cycle}

In many practical applications, also the total feed concentration can be easily modified, for example by evaporating some of the solvent from the feed solution. The total feed concentration increases while the feed composition c_1^F/c_2^F remains constant. In this case, an important practical problem is, whether a large volume of dilute sample or a small volume of concentrated sample, should be injected into the chromatography process to minimize the separation costs?

When the injected loading is held constant and the total feed concentration increased, the duration of injection decreases. The derivative of c_1^S with respect to Δt_{inj} for given loading factors can be obtained from Eq. (16). The height of the first shock depends on the loading factors and the adsorption isotherm parameters only. It is interesting to note that c_1^S is independent of Δt_{inj} , and thus also on the total feed concentration, at constant loading factors:

$$\left. \frac{\partial c_1^S}{\partial \Delta t_{\text{inj}}} \right|_{L_{f,1}, L_{f,2}} = 0 \tag{40}$$

The derivative of $t_{R,1}$ with respect to Δt_{inj} is obtained by differentiating Eq. (10), where $t = t_{R,1}$ and $c_1 = c_1^S$

$$\left. \frac{\partial t_{R,1}}{\partial \Delta t_{\text{inj}}} \right|_{L_{f,1}, L_{f,2}} = 1 \tag{41}$$

Although c_1^S is independent of the duration of injection, $t_{R,1}$ increases linearly with it. This is because, in the case of constant loading factors, a larger injection volume means a lower feed concentration, which in turn means that the first shock travels at a lower velocity before the beginning of the shock erosion x_E .

By differentiating Eq. (34) it is observed that the cycle time is independent of the duration of injection for given loading. This is because both the derivative of $t_{E,2}$ and the derivative of $t_{R,1}$ with respect to Δt_{inj} are unity

$$\left. \frac{\partial t_{\text{cycle}}}{\partial \Delta t_{\text{inj}}} \right|_{L_{f,1}, L_{f,2}} = 0 \tag{42}$$

6.5. Effect of the total feed concentration on the process performance

When the loading factors are constant and the duration of injection decreases, the amount of the product increases due to enhanced displacement effect. This has been proven analytically for the second component [20] and can be shown analogically for the first component. Because the cycle time is independent of Δt_{inj} , the productivity of both the first and the second component must decrease as the duration of injection increases. At the same time, the yield of the target component decreases since less product is obtained with same loading. This means that both the maximum productivity and the maximum yield are always achieved when the duration of injection is as small as possible and the total feed concentration is as high as possible. In practice, this usually means that the process is operated at the solubility limit. The results are congruent with the observations that in most cases the concentration overloading is a more economic approach than the volume overloading [12].

In some cases, the improvement in the productivity and yield gained by removing solvent from the feed is counter-balanced by increase in the specific eluent consumption. This is because V_{eluent} increases when the feed concentrations increase as seen by differentiating the numerator of Eq. (33). According to numerical simulations, the specific eluent consumptions go through minimum or tend towards minimum when the feed concentrations tend towards infinity. However, although the cycle time is independent of Δt_{inj} , it is not straightforward to derive a closed form equation for the zero points of derivatives $\partial EC_i / \partial \Delta t_{inj}$. This is because the slope of the Γ_+ characteristic corresponding feed state and so the rear part of the chromatogram changes when the feed concentrations change. Implicit expressions are obtained by calculating $\partial EC_i / \partial \Delta t_{inj}$ as a function of Δt_{inj} .

7. Conclusions

For decades, there has been available an exact analytic solution of the ideal model of chromatography for binary Langmuir systems that allows analytic calculation of individual elution profiles, except for the height and retention time of the first shock in the case of a narrow injection pulse. In this work, the existing solution was completed by deriving the missing closed-form equations for the height and retention time of the first shock. It was thus shown that, for binary Langmuir systems, the individual concentration profiles at column outlet can be expressed entirely in closed-form.

The height of the first shock is obtained as a root of a quartic equation, which has only one positive root. Four algorithms were compared for solving the quartic. The Ferrari's algorithm was observed to be the most stabile one.

The trajectory of the first shock in distance–time plane was discussed briefly. It was shown that the time coordinate of the first shock in the physical plane can be expressed analytically as a function of the distance from the column inlet. In addition, a novel, simple parametric representation, which gives the trajectory of the first shock as a function of shock height c_1^S , was derived.

The practical relevance of the analytic equations giving c_1^S and $t_{R,1}$ was demonstrated by using them for optimization of batch chromatography process. It was shown that c_1^S increases and $t_{R,1}$ decreases with increasing duration of injection when the feed concentrations are constant. In addition, the derivative of the cycle time with respect to Δt_{inj} is always more than unity. For this reason, the maximum productivity of component 2 is achieved when the duration of injection is selected so that the purity constraint can be fulfilled by having 100% yield. For the first component, productivity goes through a maximum, for which an implicit expression was derived.

When the injected loadings are constant, $t_{R,1}$ decreases with increasing feed concentrations. In contrast, c_1^S and Δt_{cycle} are independent of them. The maximum productivities of the components are always obtained with maximum feed concentrations, which are usually limited by viscosity or solubility.

Nomenclature

a	Henry constant
A	coefficient of the quartic term in Eq. (17)
b	Langmuir parameter, L/mol or L/g
B	coefficient of the cubic term in Eq. (17)
c	mobile phase concentration, mol/L or g/L
c_1^A	concentration of the first component at the first component plateau, mol/L or g/L
c_1^A'	concentration of the first component at the front of the second component shock, mol/L or g/L
c_i^F	concentration of component i in feed, mol/L or g/L
c_1^M	concentration of the first component at the rear of the second component shock, mol/L or g/L
c_1^S	concentration of the first component at the top of the first component shock, mol/L or g/L
C	coefficient of the quadratic term in Eq. (17)
D	coefficient of the linear term in Eq. (17)
E	constant term in Eq. (17)
EC	specific eluent consumption, L/mol or L/g
F	phase ratio
k	coefficient of the linear term in Eq. (1.1)
L	column length, m
L_f	loading factor
L_f'	auxiliary parameter, $(1 + \xi_+ b_1 / b_2) L_{f,2}$
m	constant term in Eq. (1.1)
p^j	purity of fraction j with respect to a target component
Q	auxiliary parameter defined by Eq. (1.5)
q	stationary phase concentration, mol/L or g/L
q_m	saturation capacity of the adsorbent, mol/L or g/L
PR	productivity, mol/s or g/s
R	auxiliary parameter defined by Eq. (1.10)
res	relative residual
S	auxiliary parameter defined by Eq. (1.11)
T	auxiliary parameter defined by Eq. (1.12)
u	interstitial velocity, m/s
t	time, s
t_0	elution time of a non-retained component, s
t_{cut}	cut time, ending of the collection of the first fraction and beginning of the collection of the second fraction, s
$t_{E,1}$	retention time of the end of elution profile of the first component, s
$t_{E,2}$	retention time of the end of elution profile of the second component, s
$t_{R,1}$	retention time of the front shock of the first component, s
$t_{R,2}$	retention time of the front shock of the second component, s
V	volume, L
\dot{V}	flow rate, L/s
V_{eluent}	amount of eluent used in a chromatographic cycle, L
x	axial coordinate, m
Y	recovery yield
y	a root of Eq. (1.1)

Greek symbols

α	separation factor
β	auxiliary parameter, $\beta = 1 - 1/\alpha$
Γ	characteristic of a simple wave
γ	auxiliary parameter, $\gamma = (\alpha b_1 \xi_+ + b_2) / (b_1 \xi_+ + b_2)$

Δt_{cycle}	cycle time, s
Δt_{inj}	duration of a rectangular injection pulse, s
η	auxiliary parameter defined by Eq. (B.6)
κ	auxiliary parameter defined by Eq. (B.4)
λ	auxiliary parameter defined by Eq. (B.5)
ξ_+	slope of Γ_+ characteristic corresponding feed state

Subscripts

1, 2	components to be separated
------	----------------------------

Appendix A.

In this appendix, it is shown that Eq. (16), and thus Eq. (17), has at most one positive real root and does not have any complex root with positive real part. For this purpose, Eq. (16) is rewritten as

$$f = L_{f,1} \left(1 + \frac{1}{b_1 c_1^S} \right)^2 + L_{f,2} \left(1 + \frac{1}{\alpha(1 + b_1 c_1^S) - 1} \right)^2 - 1 = 0 \quad (\text{A.1})$$

and f is differentiated with respect to c_1^S

$$\frac{\partial f}{\partial c_1^S} = -2b_1(1 + b_1 c_1^S) \left[\frac{L_{f,1}}{(b_1 c_1^S)^3} + \frac{L_{f,2}}{\alpha(1 - 1/\alpha + b_1 c_1^S)^3} \right] < 0 \quad (\text{A.2})$$

The above derivative is always negative when $b_1 > 0$, $\alpha > 1$, $L_{f,1} > 0$, $L_{f,2} > 0$, and $c_1^S > 0$. This means that the left hand side of Eq. (16) is strictly decreasing when $c_1^S > 0$, and thus Eq. (16) has at most one positive real root.

The fact that Eq. (16) does not have any complex root with positive real part can be shown by setting $c_1^S = \text{Re}(c_1^S) + \text{Im}(c_1^S)$ in Eq. (16). When the terms of the resulting equation are arranged to real and imaginary parts, it is seen that the imaginary part is always unequal to zero when $\text{Re}(c_1^S)$ is positive. This implies that the above statement is true and the right root of Eq. (16) is always the one having the largest real part.

Appendix B. Calculation of the maximum productivity of the first component

In this appendix, it is shown how to calculate the duration of injection that leads to the maximum productivity of the first component, providing that Δt_{inj} is located on the region where the first component plateau is eroded. The discussion is limited to case where the feed concentrations are fixed.

PR_1 tends towards zero, when Δt_{inj} tends towards zero or infinity. For this reason, the maximum productivity is always achieved when the derivative of the productivity with respect Δt_{inj} equals zero

$$\frac{\partial PR_1}{\partial \Delta t_{\text{inj}}} = \frac{\Delta t_{\text{cycle}}(\partial m_1^A / \partial \Delta t_{\text{inj}}) - m_1^A(\partial \Delta t_{\text{cycle}} / \partial \Delta t_{\text{inj}})}{(\Delta t_{\text{cycle}})^2} = 0 \quad (\text{B.1})$$

The above derivative can be calculated explicitly as a function of c_1^S . The cycle time is given by

$$\Delta t_{\text{cycle}} = t_0 F a_1 \left[\alpha - \frac{1}{(1 + b_1 c_1^S)^2} \right] + \frac{\beta a_1 c_2^F}{q_{m,2}(\beta + b_1 c_1^S)^2} \Delta t_{\text{inj}} \quad (\text{B.2})$$

and the mass of the first component in the product fraction A by

$$m_1^A = c_1^F \Delta t_{\text{inj}} - \lambda \left(\sqrt{\kappa + \eta \Delta t_{\text{inj}}} \right)^2 \quad (\text{B.3})$$

with

$$\kappa = \frac{(1 - p^A)}{p^A} \alpha \xi_+ \quad (\text{B.4})$$

$$\lambda = \frac{F(\gamma - 1)(a_2 - a_1)}{b_1(1 - \kappa)^2} \quad (\text{B.5})$$

$$\eta = \frac{\alpha b_2(1 - \kappa)((1 - p^A)/p^A)c_1^F - c_2^F}{F(a_2 - a_1)(\gamma - 1)} \quad (\text{B.6})$$

For the duration of injection, the following expression is obtained from Eq. (16)

$$\Delta t_{\text{inj}} = \frac{t_0 F}{(c_1^F/q_{m,1})(1 + (1/b_1 c_1^S))^2 + (c_2^F/q_{m,2})(1 + b_1 c_1^S)/(\beta + b_1 c_1^S)^2} \quad (\text{B.7})$$

The derivate of the cycle time is obtained by differentiating Eq. (B.2)

$$\frac{\partial \Delta t_{\text{cycle}}}{\partial \Delta t_{\text{inj}}} = \frac{(t_0 F a_1 / \Delta t_{\text{inj}})[(t_0 F / \Delta t_{\text{inj}})(1 + b_1 c_1^S)^3] - (\beta c_2^F / q_{m,2})(\beta + b_1 c_1^S)^3]}{(1 + b_1 c_1^S)[(c_1^F / q_{m,1})(b_1 c_1^S)^3] + (c_2^F / q_{m,2})\alpha(\beta + b_1 c_1^S)^3]} + \frac{\beta a_1 c_2^F}{q_{m,2}(\beta + b_1 c_1^S)^2} \quad (\text{B.8})$$

and the derivative of m_1^A by differentiating Eq. (B.3)

$$\frac{\partial m_1^A}{\partial \Delta t_{\text{inj}}} = c_1^F - \lambda \left(\eta - \frac{\eta}{\sqrt{\kappa + \eta \Delta t_{\text{inj}}}} \right) \quad (\text{B.9})$$

Eq. (B.1) remains implicit with respect to c_1^S and must be solved numerically. Once c_1^S is obtained, the corresponding Δt_{inj} is calculated from Eq. (B.7). If Eq. (B.1) has no roots between 0 and c_1^A , the maximum productivity lies on the region where the first component plateau is not eroded.

Appendix C. Supplementary data

A Matlab code that calculates individual concentration profiles at column outlet analytically, to be used for non-commercial purposes, can be obtained from the publisher's website. Use command `ideal_model_binary_Langmuir(help)`; to display instructions. The code requires Matlab version 7.5 (Matlab R2007b) or newer to run.

Supplementary data associated with this article can be found, in the online version, at [doi:10.1016/j.chroma.2011.07.004](https://doi.org/10.1016/j.chroma.2011.07.004).

References

- [1] F. Helfferich, G. Klein, Multicomponent Chromatography. Theory of Interference, Marcel Dekker, New York, 1970.
- [2] D. Devault, J. Am. Chem. Soc. 65 (1943) 532.
- [3] E. Glueckauf, Discuss. Faraday Soc. 7 (1949) 12.
- [4] H.-K. Rhee, R. Aris, N.R. Amundson, Philos. Trans. R. Soc. Lond. Ser. A 267 (1970) 419.
- [5] S. Golshan-Shirazi, G. Guiochon, J. Phys. Chem. 93 (1989) 4143.
- [6] S. Golshan-Shirazi, G. Guiochon, J. Chromatogr. 484 (1989) 125.
- [7] H.-K. Rhee, R. Aris, N.R. Amundson, First-Order Partial Differential Equations. Theory and Application of Single Equations, vol. I, Dover Publications, New York, 2001.
- [8] H.-K. Rhee, R. Aris, N.R. Amundson, First-Order Partial Differential Equations. Theory and Application of Hyperbolic Systems of Quasilinear Equations, vol. II, Dover Publications, New York, 2001.
- [9] A. Rajendran, M. Mazzotti, Ind. Eng. Chem. Res. 50 (2011) 352.
- [10] S. Golshan-Shirazi, G. Guiochon, Anal. Chem. 61 (1989) 1276.
- [11] S. Golshan-Shirazi, G. Guiochon, Anal. Chem. 61 (1989) 1368.
- [12] G. Guiochon, A. Felinger, D.G. Shirazi, A.M. Katti, Fundamentals of Preparative and Nonlinear Chromatography, 2nd ed., Academic Press, Amsterdam, 2006.
- [13] T. Sainio, M. Kaspereit, Sep. Purif. Technol. 66 (2009) 9.
- [14] G. Storti, M. Mazzotti, M. Morbidelli, S. Carra, AIChE J. 39 (1993) 471.
- [15] M. Kaspereit, A. Seidel-Morgenstern, A. Kienle, J. Chromatogr. A 1162 (2007) 2.
- [16] A. Rajendran, W. Chen, Sep. Purif. Technol. 67 (2009) 344.
- [17] W.H. Beyer (Ed.), CRC Standard Mathematical Tables, CRC Press, Boca Raton, Florida, 2000.
- [18] R.S. Burington, Handbook of Mathematical Tables and Formulas, 5th ed., McGraw-Hill, New York, 1973.
- [19] S. Neumark, Solution of Cubic and Quartic Equations, Pergamon Press, Oxford, 1965.
- [20] J. Siitonen, T. Sainio, M. Kaspereit, Sep. Purif. Technol. 78 (2011) 21.